

A Power Spectral Density Study of Thin Films Morphology Based on AFM Profiling

R. GAVRILA¹, A. DINESCU¹, D.MARDARE²

¹R&D Institute for Microtechnology – Bucharest, Romania
E-mail: ralucag@imt.ro

²Faculty of Physics, Al. I. Cuza University, Iași, Romania
E-mail: dianam@uaic.ro

Abstract. *Atomic Force Microscopy* (AFM) is extensively being used for characterizing thin film surfaces. In addition to direct imaging, AFM profile data enable to derive the *Power Spectral Density* (PSD) of the surface roughness and thus provide useful information on characteristic features which compose the microstructure of the films. In the present work PSD spectra computed from AFM data were used for studying the morphology of three different titanium oxide thin films obtained by dc magnetron sputtering onto glass. The derived PSD curves were fitted with an appropriate analytic function and characteristic parameters were deduced and discussed in order to compare film morphologies in conjunction with the deposition conditions.

1. Introduction

Currently there is a great interest in designing and engineering thin films with morphologies tailored to specific requirements for various application fields. The connection between surface morphology of the films and functionality is especially important for optical applications, as surface microstructure generates scattering and stray light in optical components.

The most popular parameter characterizing the morphology of surfaces is the rms roughness σ , which represents the root mean square height of a surface around its mean value. However this statistical description, though simple and reliable, makes no distinction between peaks and valleys and does not account for the lateral distribution of surface features. A more complete description is provided by the power

spectral density (PSD) of the surface topography, which performs a decomposition of the surface profile into its spatial wavelengths and allows comparison of roughness measurements over different spatial frequency ranges. For optical surfaces the PSD function is especially important and represents a very popular way to describe the surface quality as it is connected with the amount and angular repartition of scattered light. Thereby scattering theories predict that in the smooth-surface limit the angular distribution of light scattered from a surface fits the power spectral density (PSD) of the surface topography [1]:

$$IS(\theta, \phi) = C(\theta, \phi) \cdot PSD(f_x, f_y) \quad (1)$$

where $IS(\theta, \phi)$ is the scattered flux per solid angle unit in the (θ, ϕ) direction, $PSD(f_x, f_y)$ is the 2-D PSD of the surface topography, f_x, f_y are the spatial frequencies, related to the incident (θ_i) and scattering (θ, ϕ) angles, $C(\theta, \phi)$ is an optical factor which depends on the refraction indexes of the incident medium (generally air) and surface material and on the illuminating and observation conditions (wavelength, geometry, polarization).

This study focuses on titanium oxide, a material currently used as thin film coating in optical applications due to its notable dielectric and optical properties. Owing to their good durability, stability and high refractive index, TiO_2 thin films are used as antireflection coatings [2], optical filters (in multilayer coatings) [3], optical wave-guides [4] and recently, due to its semiconducting properties, as photocatalytic coatings in anti-fogging mirrors [5].

2. Definitions

Different methods for computing PSD from profiling data are found in literature, most of them differing by normalization procedures. This fact encumbers the reference and comparison of results and urges for the specification of the PSD expressions used in each case.

In this work we have adopted the following definition for the 2-D PSD of a surface described by its topography $z(x, y)$:

$$S_2(f_x, f_y) = \lim_{L \rightarrow \infty} \frac{1}{L^2} \left\{ \int_{-1/2L}^{1/2L} dx \int_{-1/2L}^{1/2L} dy \cdot z(x, y) \cdot \exp[2\pi i(f_x \cdot x + f_y \cdot y)] \right\}^2 \quad (2)$$

where L is the scan length, assumed to be equal in x and y directions, f_x, f_y are the spatial frequencies (inverse of spatial wavelengths) for x and y directions, respectively, and $i = \sqrt{-1}$.

Strictly speaking, the integral in expression (2) is not exactly the Fourier transform of the height function $z(x, y)$, as the existence of the limit depends on the properties of the function and moreover the limit $L \rightarrow \infty$ is physically unattainable. In practice

a finite N number of values are measured, assumed to be equidistantly spaced in x, y directions at distances $\Delta x, \Delta y = L/N$. The 2-D PSD is then computed as:

$$S_2(f_x, f_y) \approx L^2 \left[\frac{1}{N^2} \sum_{n=0}^N \sum_{m=0}^N z(x_m, y_n) \exp(2\pi i \cdot x_m \cdot f_x) \cdot \exp(2\pi i \cdot y_n \cdot f_y) \right]^2 \quad (3)$$

where $x_m = m \cdot \frac{L}{N}$, $y_n = n \cdot \frac{L}{N}$, and the spatial frequencies f_x, f_y take the discrete range of values:

$$f_x, f_y = \frac{1}{L}, \frac{2}{L}, \dots, \frac{N}{2L}.$$

The analogous PSD definition for the 1-D case, corresponding to the topography of a profile described by its height $z(x)$ is:

$$S_1(f_x) \approx L \left[\frac{1}{N} \sum_{k=1}^N z_k \cdot \exp(2\pi i \cdot x_k \cdot f_x) \right]^2, \quad (4)$$

with $x_k = k \cdot \frac{L}{N}$ and $f_x = j \cdot \frac{1}{L}$, $j = 1, 2, \dots, \frac{N}{2}$.

3. Experiment

Three titanium oxide films were deposited onto glass substrates by d.c. magnetron-sputtering method, using water vapors as reactive gas, with the same deposition rate, $r = 0.02$ nm/s. After deposition all samples were submitted to a thermal treatment within a certain temperature range ΔT . The experimental arrangement and deposition technique are described in [6].

The samples, denoted L31, L48 and L27, differ by substrate temperature during deposition and film thickness, as shown in Table 1.

Table 1

sample	L31	L48	L27
substrate temperature [°C]	310	480	270
film thickness [nm]	450	260	230

The investigations described in [6] showed that the deposited titanium oxide films have a polycrystalline and generally multiphasic (anatase and/or rutile) structure. The samples L27 and L31 have a mixed crystalline structure with an equal proportion of anatase and rutile, while pure rutile structure has been observed for the sample L48.

The morphology of the films, together with that of the uncoated glass substrate were measured with a home-built Atomic Force Microscope (AFM) operated in contact mode. For each sample $1 \mu\text{m} \times 1 \mu\text{m}$ and $10 \mu\text{m} \times 10 \mu\text{m}$ scans were performed, using silicon nitride cantilevers with sharpened pyramidal tips, nominal tip radius of 20 nm and nominal apex angle of 18° . The tip shape was checked after each measurement with the aid of reference samples and SEM imaging. These checks have shown

that tip radius increased during the $10\ \mu\text{m} \times 10\ \mu\text{m}$ measurements. Actually it was almost impossible to maintain the initial tip shape intact over a full $10\ \mu\text{m}$ scan, because of the strong tendency of the tip to wear, especially in the scanning direction. In Fig. 1 is purposely shown the SEM image of an initially sharp tip, severely worn in the direction parallel to the scan after a $10\ \mu\text{m} \times 10\ \mu\text{m}$ measurement.

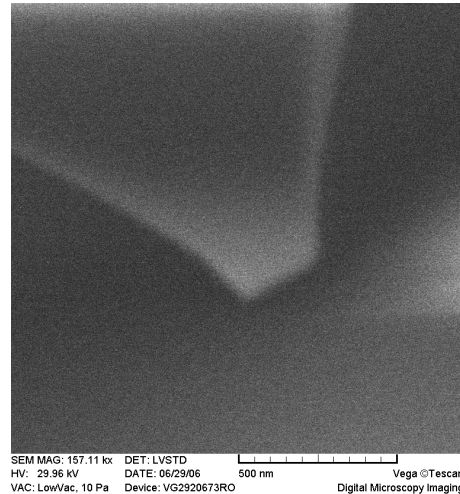


Fig. 1. $157\ 000\times$ magnification SEM image of the apex region of a tip, severely damaged in the direction parallel to the scan; the tip sharpness was quite unaffected in the direction normal to the scan.

Due to that phenomenon each sample was measured several times with different new tips and the image acquired with the less affected tip was retained for subsequent processing.

4. Data processing

An important step for obtaining consistent results is the correction of the instrumental AFM artifacts generally due to the piezo scanner, artifacts which could mask the real surface morphology. For that purpose, all raw data sets were subjected to a similar procedure meant to remove plane artifacts (tilt and bow) and occasional noise or contamination that can cause the scan lines to be leveled differently. This procedure consisted in a global flattening correction by a three order polynomial fit and a line by line correction by least mean square and histogram alignment methods. Image and data processing were done with SPIP™ software.

Although with great value in optical applications, the 2-D PSD of the surface morphology is difficult to work with and unpractical for comparing purposes. In order to condense the acquired information and facilitate the comparison between the samples, a 1-D PSD could be extracted from the 2-D function. It is this approach that we have taken in the present work.

Scans made by rotating the samples in different directions were practically identical, so it could be assumed that the films are isotropic; the natural procedure for 1-D PSD extraction would be in this case the transition to polar coordinates in frequency space and angular averaging. But in AFM measurements the data acquired in y (slow scan) direction are usually distorted by instrumental drift and moreover in this case by the asymmetrical tip geometry. This slight apparent deviation from perfect isotropy could be noticed in Fig. 2, an image of the 2-D PSD for the sample L31 given for exemplification.

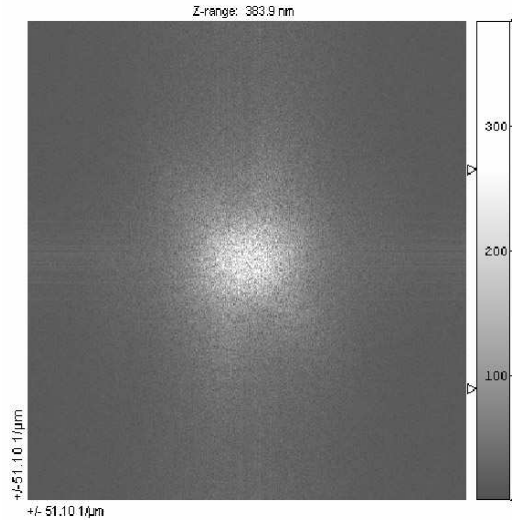


Fig. 2. 2-D PSD plotted for the surface morphology of L31.

For that reason we have preferred to compute the 1-D PSD function $\overline{S_1}(f_x)$ obtained by integrating $S_2(f_x, f_y)$ defined by Eq. (3) over f_y .

It can be shown [7] that $\overline{S_1}(f_x)$ essentially represents the average over y of the 1-D PSD $S_1(f_x, y)$ computed according to Eq. (4) from profiles traced in x (fast scan) direction:

$$\overline{S_1}(f_x) \approx \frac{1}{N} \sum_{n=1}^N S_1(f_x, y_n). \quad (5)$$

In order to increase the frequency range of the resulting PSD, two sets of calculations were performed, based on $10 \times 10 \mu\text{m}^2$ scan size, respectively $1 \times 1 \mu\text{m}^2$ scan size. For a better statistic two to four data sets obtained from different locations of the samples were processed and then averaged for each case. Because of the tip predisposition to blunt in the much wearing $10 \mu\text{m}$ scans, the shorter wavelength region (magnitudes comparable to estimated tip radius) of the PSD curves obtained from these scans were set aside in subsequent calculations. Finally the PSDs computed from $10 \times 10 \mu\text{m}^2$ scans and $1 \times 1 \mu\text{m}^2$ scans were properly combined for every sample to give the extended PSD.

5. Results and discussion

Figure 3 a–d displays the surface morphology of the uncoated glass substrate and respectively of L31, L48 and L27 thin film samples.

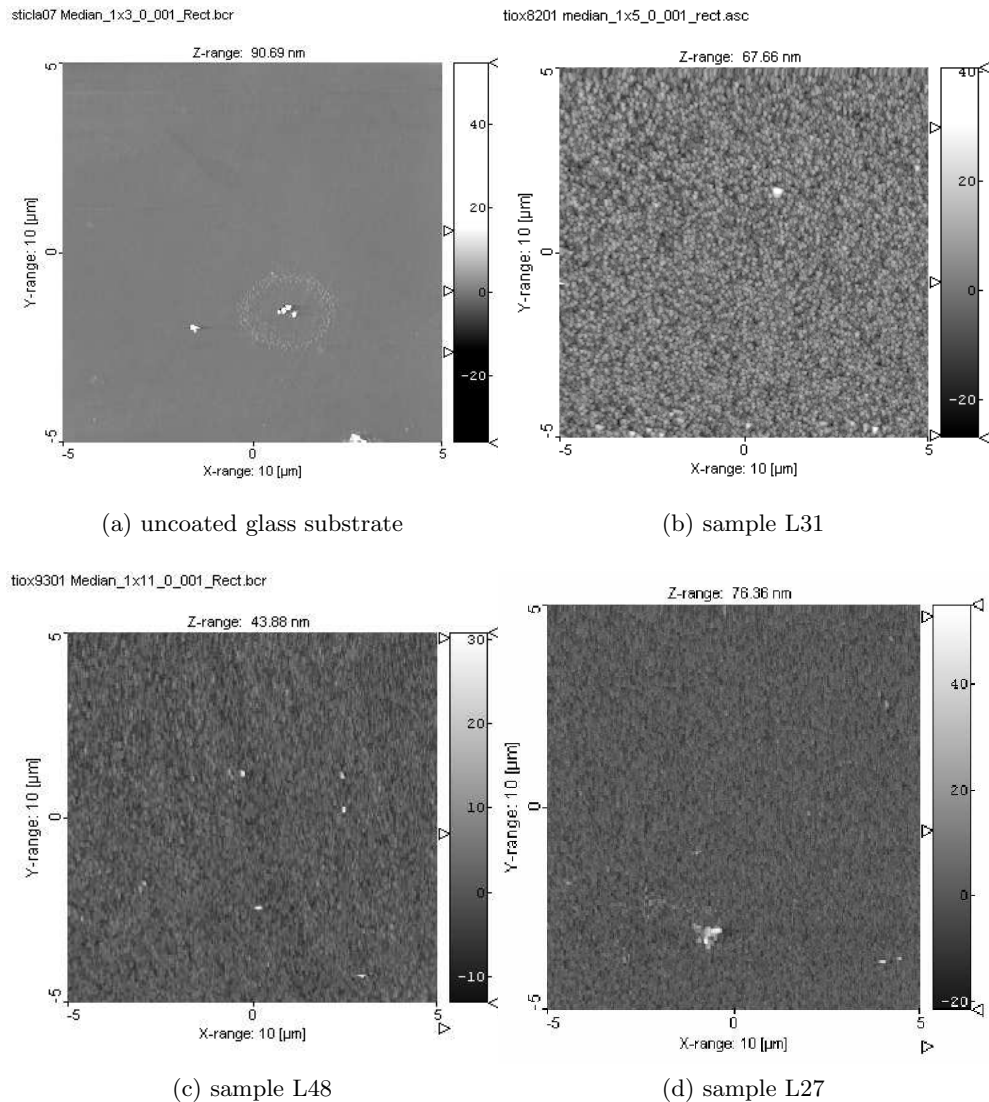


Fig. 3. AFM images of the surface morphology of substrate and titanium oxide thin films. Scan area $10 \times 10 \mu\text{m}^2$.

In Fig. 4 the fine-grained structure of thin film samples is more explicitly revealed in the $1 \times 1 \mu\text{m}^2$ images. The larger grains in the structure of L31 film compared with L48 and L27 films could be easily perceived.

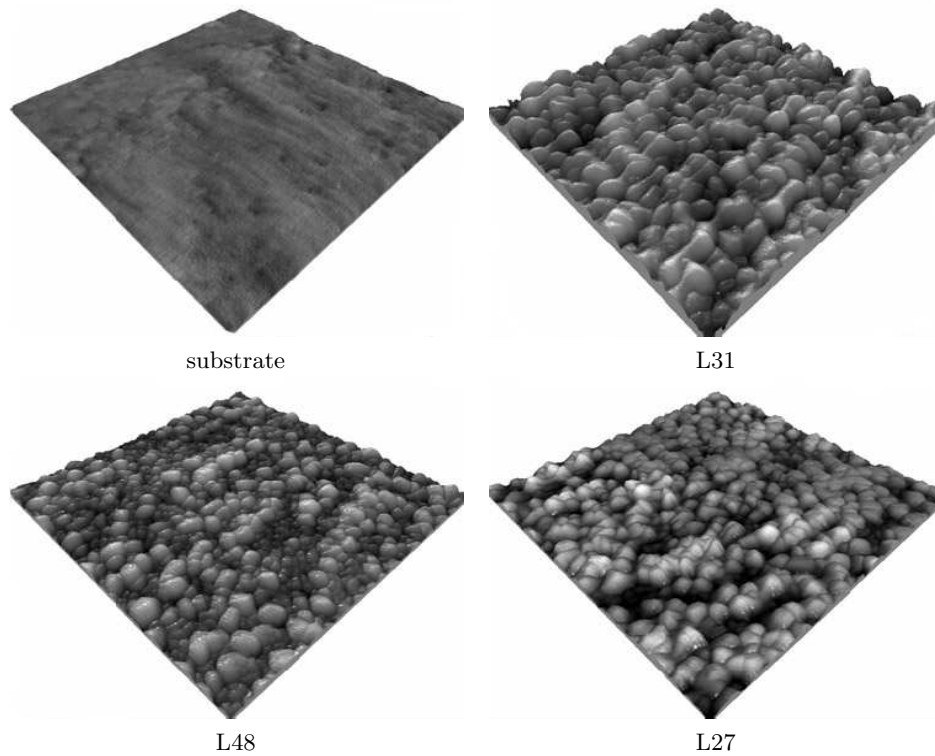


Fig. 4. $1 \times 1 \mu\text{m}^2$ AFM images of the substrate and titanium oxide samples, displaying the granularity of the films.

Table 2 contains the rms roughness values for the films and glass substrate, computed for the 1×1 scans in order to avoid the influence of the large casual defects which appear in the $10 \times 10 \mu\text{m}^2$ images (see Fig. 3).

Table 2

	uncoated glass	L31	L48	L27
rms roughness (nm) for $1 \mu\text{m}^2$	1.0	7.0	3.3	4.4

Figure 5 displays in a log-log plot the resulted PSD profiles computed by the technique described in the previous section for the three samples, together with that for the substrate.

As one can see, all PSD curves essentially present the same characteristic shape, consisting in a flat response in the lower part of the spatial frequency spectrum and a power law roll-off with frequency in the upper part of the spectrum. The strong spikes in the mid and high frequency range of the substrate PSD were neglected in the presents study, as additional work is needed to elucidate if they correspond to real periodicities of the surface morphology or to measurement artifacts and/or noise.

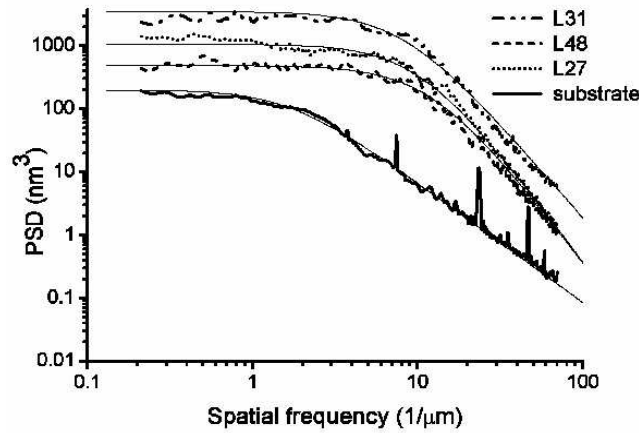


Fig. 5. PSD profiles of thin film samples and substrate, calculated from AFM measurements, displayed together with their ABC-model fits.

The curves depicted in Fig. 5 clearly indicate that over the entire spectrum of frequencies the thin film morphology dominates the substrate morphology for all the samples. It is to be mentioned that in the range of spatial frequencies which come into play for optical (visible and UV) scattering, for all the films the roughness is quasi uniformly distributed with frequency (white spectrum); the slight deviation of L27 at low frequencies will be discussed below. Considering the topographic scattering in optical applications, it is obvious that this would not be influenced by improving the substrate finish and scatter reduction could be achieved only by changing the deposition conditions, both for visible and UV regions.

The steadiness and relative smoothness of the thin films PSD curves, their quasi-alignment in the low spatial frequency zone and their monotonic ranking with respect of the roughness (in descending order L31, L27, L48) over the whole range of frequencies suggest a similar overall mechanism underlying film growth for all samples.

For a condensed description of the thin film and substrate morphology, we made use of the so-called ABC of k-correlation model, which proved to be applicable to a large range of sample morphologies and allows quantitative comparison between samples over large length scales [1]:

$$S(f) = \frac{A}{[1 + (B \cdot f)^2]^{\frac{C}{2}}}, \quad (6)$$

where A, B and C are model parameters.

A is the value of the spectrum in the low-frequency limit, the “shoulder parameter” B is a “correlation length” which sets the point of the transition between the low and high-frequency behavior, and C is the exponent of the power-law fall-of f at high frequencies. At low spatial frequencies ($f \ll 1/B$) the PSD is constant and equals A; at high f values, the surface is fractal, its PSD function scaling as $1/f^C$. This model

can be seen as a generalization of the fractal case (pure roll-off of PSD with increasing frequency), with a flat response below a cut-off frequency.

As shown in Fig. 5, the ABC model succeeds in describing quite satisfactory the morphologies for both the substrate and all thin film samples over the entire spatial frequency range. The A, B and C parameters of the respective fits are given in Table 3:

Table 3

	substrate	L31	L48	L27
A (nm ³)	200	3500	482	1066
B (nm)	595	123	82	96
C	1.9	3	3.4	3.5

Several observations could be drawn from the above results:

- In the mid and high frequency regions, the glass substrate behaves as an ideal fractal surface ($C \sim 2$).

- The value of A parameter is related to the low frequency component of surface roughness, while the value of B parameter (the correlation length), is linked to grain size.

- The roughness value increases with the grain size. For L31 and L27 films, which have about similar phase composition, grain size (and roughness) enhances with increasing film thickness and substrate temperature. Slightly smaller grain size (smaller B) and consequently smaller roughness seem to characterize pure rutile phase, obtained with the greater substrate temperature (sample L48) in comparison to mixed rutile and anatase phases of L31 and L27.

- While at high spatial frequencies the roughness values of L48 and L27 tend to converge, their PSD curves move away as the frequency lowers. This behavior is reflected by the similarity of B (grain size) and C (power exponent) and by the considerable difference of A values. The low frequency upper deviation of L27 SD from the ABC model may be attributed to the presence of large scale structures (aggregates) [8] in a greater number in L27 than in L48, which is consistent with the lower substrate temperature during deposition for L27.

6. Conclusions

The main goal of this work was to establish and test a procedure for computing and combining PSD spectra from AFM data acquired on different length scales on optical surfaces. This procedure was applied for studying the morphology of three different thin titanium oxide films obtained by dc magnetron sputtering. This type of study provides a more comprehensive understanding of the influence of the obtaining conditions on morphological features of the films and could help in tailoring the deposition parameters according to surface morphology requirements for a specific application. Particularly, as for optical thin films PSD is closely linked to the bidirectional reflectance distribution function (BRDF), AFM data can support optimization of the obtaining processes with the view of reducing scatter losses in thin film optical coatings.

References

- [1] CHURCH E. L., TAKACS R. Z., 7. *Surface Scattering*, in *Handbook of Optics* (2nd ed), vol. I, *Fundamentals, Techniques and Design*, McGraw Hill, New York, 1995.
- [2] BANGE K. et al., *Thin Solid Films*, **197**, p. 279, 1991.
- [3] SAWADA Y., TAGA Y., *Thin Solid Films*, **116**, p. 155, 1984.
- [4] SIEFERING K. L., GRIFFIN G. L., *J. Electrochem. Soc.*, **137**, p. 1206, 1990.
- [5] Annual Report 2003, Fraunhofer-Institut für Silicatforschung ISC.
- [6] MARDARE D., BABAN C., GAVRILA R., MODREANU M., RUSU G. I., *Surface Science*, **507**, pp. 468–472, 2002.
- [7] MARX E. et al., *J. Vac. Sci. Technol. B*, **20**(1), pp. 31–41, 2002.
- [8] SENTHILKUMAR M. et al., *Applied Surface Science*, **252**, pp. 1608–1619, 2005.